Available online at www.sciencedirect.com
SCIENCE DIRECT®
European Journal of Pharmacology 467 (2003) 31–39
www.elsevier.com/locate/ejphar

A phenylacetate derivative, SCK6, inhibits cell proliferation via G_1 cell cycle arrest and apoptosis

Hsu-Chin Chan[a,b], Sheng-Chu Kuo[b], Li-Jiau Huang[b], Chung-Hsien Liu[c], Shih-Lan Hsu[d,*]

[a] *Department of Biochemistry, China Medical College, Taichung, Taiwan, ROC*
[b] *Graduate Institute of Pharmaceutical Chemistry, China Medical College, Taichung, Taiwan, ROC*
[c] *School of Medicine, Chung Shan Medical University, Taichung, Taiwan, ROC*
[d] *Department of Medical Research, Taichung Veterans General Hospital, Taichung, Taiwan, ROC*

Received 17 October 2002; received in revised form 28 February 2003; accepted 7 March 2003

Abstract

Phenylacetate is a differentiation agent and has anticancer activity with relatively low toxicity. In the present study, we examined the anticancer effect of six synthetic phenylacetate derivatives in human lung cancer cells in our search for more effective phenylacetate analogous. Results showed that the antiproliferative effects of these synthetic compounds were stronger than those of phenylacetate, and that *N*-butyl-2-(2-fluorolphenyl)acetamide (SCK6) is the most potent compound. To address the mechanism of the antiproliferative effect of SCK6, cell cycle analysis was performed. Result showed that SCK6 (1 mM) induced G_1 arrest in CH27 cells. Western blot analysis of G_1 phase regulatory proteins demonstrated that the protein levels of cyclin-dependent kinase 2 (Cdk2), Cdk4, Cyclin E and Cyclin D3 were decreased after treatment with SCK6 but not those of Cdk6, Cyclin D1 and D2. In contrast, SCK6 increased the protein levels of p53 and $p21^{CIP1/WAF1}$. Data from in situ terminal transferase-mediated dUTP-fluorescensin nick end-labeling (TUNEL) assay and DNA fragmentation analysis demonstrated that SCK6 induced apoptotic cell death in CH27 cells. This SCK6-induced apoptosis was accompanied by a downregulation of Bcl-2 protein and activation of the caspase-9 cascade. Overexpression of Bcl-2 by adeno-Bcl-2 vector infection significantly inhibited SCK6-induced apoptosis. Moreover, treatment with caspase inhibitors also markedly reduced cell death induced by SCK6. Taken together, these results suggest that downregulation of G_1-associated Cdks and cyclins and upregulation of p53 and $p21^{CIP1/WAF1}$ may contribute to SCK6-mediated G_1-phase arrest. Furthermore, the decrease in Bcl-2 and the activation of caspase-9/caspase-3 may be the effector mechanism through which SCK6 induces apoptosis.

Keywords: Phenylacetate derivative; Cell cycle; Caspase; Apoptosis

1. Introduction

Lung cancer is the leading cause of cancer death in Taiwan and throughout the world in both developed and developing countries. Patients with lung cancer are often treated by surgery followed by radiotherapy and chemotherapy (Kotas et al., 2001; Semik et al., 2001). However, the 5-year survival rate for lung cancer in Taiwan is only 5–8% (Wu, 1998). Clearly, new therapeutic agents are needed for the treatment of these patients. Compounds that induce growth arrest and differentiation may provide an attractive alternative in cases where cytotoxic therapy or hormonal manipulation is not effective. Small molecules such as aromatic fatty acids were recently proposed as a new class of tumor growth-inhibitory compounds. Phenylacetate, a physiological product of phenylalanine metabolism, is present in micromolar concentrations in human plasma (Cosentini et al., 2001; Sandler et al., 1982). It has been shown that phenylacetate is a nontoxic differentiation inducer and has antiproliferative effects against several cancer cells (Samid et al., 1992a,b, 1993; Cinatl et al., 1993, 1994; Sidell et al., 1995). Phenylacetate and analogues have already been established as safe and effective in the treatment of hyperammonemia (Hudgins et al., 1995; Brusilow et al., 1984; Simell et al., 1986), and these drugs have been tested in clinical trials for the treatment of human

* Corresponding author. Department of Education and Research, Taichung Veterans General Hospital, No. 160, Section 3, Chung-Gang Road, Taichung, Taiwan, ROC. Tel.: +886-4-23592525x4037; fax: +886-4-23592705.
E-mail address: h2326@vghtc.vghtc.gov.tw (S.-L. Hsu).

0014-2999/03/$ - see front matter © 2003 Elsevier Science B.V. All rights reserved.
doi:10.1016/S0014-2999(03)01596-6

cancers. Phase I studies with phenylacetate confirmed that millimolar levels can be achieved in plasma and cerebrospinal fluid without any significant toxicity, and result in clinical improvement in patients with high-grade gliomas and hormone-refractory prostate cancer (Hudgins et al., 1995; Thibault et al., 1994, 1995). However, rather large doses (300 mg/kg/day or more) of phenylacetate are required to achieve therapeutic levels. This prompted us to find a more potent analogue of phenylacetate, and several phenylacetate derivatives (Fig. 1) were synthesized by Dr. Kuo and Dr. Huang.

It has been demonstrated that phenylacetate is able to induce G_1 arrest in several types of cancer cells by affecting the cell cycle regulatory proteins (Onishi et al., 2000). Phenylacetate also effectively induced apoptosis in malignant cells (Gore et al., 1997). The cell cycle in eukaryotes is regulated through a precise balance of positive and negative regulatory components that exert their effects during the G_1 phase. The most critical positive-acting components are G_1 cyclins (Cyclin Ds and Cyclin E) and cyclin-dependent kinases (Cdks) (Hunter, 1993; Sherr, 1993). In addition, some Cdk inhibitors (CdkIs) have been identified, and two groups of mammalian CdkIs are known to date: one group is the Cdk-interaction protein/Cdk inhibitor (CIP/KIP) family, including $p21^{CIP1/WAF1}$, $p27^{KIP1}$ and $p57^{KIP2}$, and has a broad specificity (Sherr and Roberts, 1995; Brugarolas et al., 1995), and the other group acts as inhibitors of the Cdk4 (INK4) family including $p15^{INK4B}$, $p16^{INK4A}$, $p18^{INK4C}$ and $p19^{INK4D}$ (Sherr and Roberts, 1995). INK4 binds only to Cdk4 and Cdk6, while CIP/KIP targets a broader range of substrates, including Cyclin D-, E- and A-dependent kinases. In spite of growth inhibition, apoptosis is also an important determinant of the response of tumors to chemotherapeutic agents (Dubrez et al., 1995). Morphological features of apoptosis include chromatin condensation, cell shrinkage, nuclear fragmentation and blebbing with the formation of membrane-bound "apoptotic bodies". These events are the result of complex cellular biochemical pathways (Vaux and Korsmeyer, 1999). Accumulating evidence indicates that members of the Bcl-2 family can be regarded as regulators of the apoptotic response, whereas the caspases function as effectors, particularly in the execution phase of the cascade of events leading to cell death.

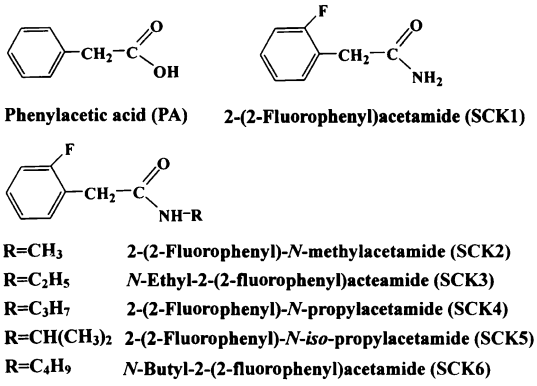

Fig. 1. Structure of phenylacetate and 2-fluorophenylacetamides with different *N*-substituted alkyl chain lengths.

In this study, we evaluated the antiproliferative activity of six synthetic phenylacetate analogues. We show here that these analogues had an enhanced potency in inducing cytostasis and apoptosis. Our preliminary results showed that *N*-butyl-2-(2-fluorolphenyl)acetamide (SCK6) is the most potent of the tested compounds. Thus, we used the human lung squamous carcinoma CH27 cell line to explore how SCK6 modulated the cell cycle and examined the relationship between the apoptotic response and molecular parameters related to the Bcl-2 family, p53 and caspase pathways. We showed that the SCK6-induced cell cycle arrest in G_1 phase correlated with the downregulation of Cdk2 and Cdk4 protein expression and the upregulation of p53 and $p21^{CIP1/WAF1}$ expression. Moreover, a decrease in Bcl-2 protein levels and activation of the caspase cascade were involved in SCK6-induced apoptotic death in CH27 cells.

2. Materials and methods

2.1. Reagents

Stock solutions of phenylacetate and *N*-alkyl-2-(2-fluorophenyl) acetamides were prepared in dimethyl sulfoxide (DMSO). Further dilutions were made immediately prior to each experiment so as not to exceed 0.25% DMSO in the culture medium. A previous study showed that 0.5% DMSO solution had no effect in cytotoxic assays (Wang et al., 2000). Phenylacetic acid was obtained from Merck–Schuchardt. The following antibodies were obtained from Santa Cruz: anti-Bcl-2, anti-Bax, anti-Bcl-X_L, anti-CDK6, anti-Cyclin A, anti-Cyclin D2 and anti-Cyclin E. Anti-$p21^{CIP1/WAF1}$, anti-p53, anti-pRb, anti-Cdk2, anti-Cdk4, anti-Cyclin D1 and anti-Cyclin D3 were purchased from Transduction Laboratories. Anti-caspase-3 and anti-cytochrome *c* were purchased from Pharmingen. 4,6-Diamidino-2-phenylindole (DAPI) and other reagents were obtained from Sigma. Caspase substrates were purchased from Biosource International QCB. z-Val-Ala-Asp-fluoromethylketone (z-VAD-fmk) was obtained from Kaymia Biomedical.

2.2. Cell culture and viability assay

Human lung squamous carcinoma CH27 cell line was provided by Veterans General Hospital Taipei, Taiwan. Cultures were in RPMI 1640 medium containing with 5% fetal bovine serum/glutamine/antibiotics, at 37 °C in 5% CO_2 humidified atmosphere. The medium was changed every 2 days. For viability assay, cells were seeded at a density of 5×10^4 cells/well in 12-well culture plates. After 24 h, cells were treated with various concentrations (0.02–2 mM) of drugs. Cell number was counted daily, using the Trypan blue dye exclusion method.

2.3. Morphological assessment of cell death

CH27 cells were treated with 1 mM phenylacetate or SCK6 for 72 h, then washed with phosphate-buffered saline (PBS) twice, fixed in 2% paraformaldehyde for 30 min and then permeabilized with 0.1% Triton X-100/PBS for 10 min at room temperature. After washing with PBS, terminal transferase-mediated dUTP-fluorescensin nick end-labeling (TUNEL) assay was performed according to the manufacturer's instructions (Boehringer Mannheim). Cells were incubated in TUNEL reaction buffer in a 37 °C humidified chamber for 60 min in the dark, then rinsed twice with PBS and incubated with DAPI (1 μg/ml) at 37 °C for 30 min. Stained cells were visualized using a fluorescence microscope. TUNEL-positive cells were counted as apoptotic cells.

2.4. DNA fragmentation

CH27 cells were treated without or with 1 mM phenylacetate or SCK6 for 72 h, and then resuspended in lysis buffer (50 mM Tris, pH 7.5, 10 mM EDTA, and 0.3% Triton X-100) for 30 min on ice. Cell lysates were treated with RNase (100 μg/ml) for 30 min at 55 °C and then treated with proteinase K (400 μg/ml) for another 1 h at 55 °C. The supernatant was extracted with phenol/chloroform. The DNA was precipitated and electrophoresed on 2% agarose gels.

2.5. Flow cytometry

CH27 cells were treated without or with 1 mM phenylacetate or SCK6 and harvested at different times. After washing with PBS, the cells were fixed in 80% ethanol/PBS for 30 min on ice. Approximately 4×10^5 cells were centrifuged and the cell pellets were re-suspended with PBS and further treated with RNase (DNase free, 100 μg/ml, final concentration in PBS) and propidium iodide (40 μg/ml, final concentration in PBS) at room temperature for 30 min. The cells were centrifuged and the cell pellets were re-suspended with PBS. The cell suspension was passed through a 19-gauge needle and kept on ice until analysis. The number of cells in different phases of the cell cycle was analyzed using a FACScan Flow cytometer with Cell-FIT software (Becton Dickinson Instruments).

2.6. Western blot analysis

CH27 cells were treated with phenylacetate or SCK6 for the indicated times. After incubation, cells were lysed in protein lysis buffer (50 mM Tris pH 7.4, 150 mM NaCl, 1 mM EDTA, 1 mM EGTA, 5% 2-mercaptoethanol, 1% Nonidet P-40, 0.25% sodium deoxycholate, 5 μg/ml leupeptin, 5 μg/ml aprotinin, 10 μg/ml soybean trypsin inhibitor, 0.2 mM phenylmethyl sulfonylfluoride); protein concentrations were determined using the Bradford method. Equal amounts of sample lysate were separated by sodium dodecylsulfate-polyacrylamide gel electrophoresis (SDS-PAGE) and electrophoretically transferred onto polyvinylidene difluoride (PVDF) membranes (Millipore). The membrane was blocked with 5% nonfat dry milk in TBST buffer (20 mM Tris, pH 7.4, 150 mM NaCl, 0.1% Tween-20), and incubated overnight at 4 °C with specific primary antibodies. Subsequently, the membrane was washed with TBST buffer and incubated with horseradish peroxidase-conjugated secondary antibodies. Determinations were performed using enhanced chemiluminescence kits (Amersham, ECL Kits).

2.7. Caspase activity assay

Caspase activity was measured by the fluorometric assay following the manufacturer's instructions. Briefly, untreated, phenylacetate- or SCK6-treated cells were incubated for the indicated times and then harvested. Cells were washed twice with ice-cold PBS and lysed in buffer (50 mM Tris, pH 7.4, 150 mM NaCl, 1 mM EDTA, 1 mM EGTA, 1 mM DL-dithiothreitol, 1% Nonidet P-40, 0.25% sodium deoxycholate, 5 μg/ml leupeptin, 5 μg/ml aprotinin, 10 μg/ml soybean trypsin inhibitor, 0.2 mM phenylmethylsulfonylfluoride). Lysates were centrifuged at $10{,}000 \times g$ for 30 min at 4 °C. Caspase activity in the supernatant was determined by a fluorogenic assay. Briefly, 20 μg of total protein was diluted in extraction buffer at a final volume of 100 μl in a microtiter plate containing 100 μM of the fluorogenic peptide substrates Ac-Tyr-Val-Ala-Asp-7-amido-4- methylcoumarin (Ac-YVAD-AMC), Ac-Asp-Glu-Val-Asp-AMC (Ac-DEVD-AMC), Ac-Ile-Glu-Thr-Asp-AMC (Ac-IETD-AMC) and Ac-Leu-Glu-His-Asp-AMC (Ac-LEHD-AMC) in 50 μl of caspase assay buffer containing 40 mM HEPES (pH 7.4), 20% glycerol (v/v), 1 mM EDTA, 0.2% NP-40 and 10 mM DL-dithiothreitol. Following incubation at 37 °C for 2 h, the release of 7-amido-4-methylcoumarin (AMC) was measured using a fluorescence spectrophotometer excitation at 360 nm and emission at 460 nm.

2.8. Determination of cytochrome c

For determination of cytosolic cytochrome *c*, CH27 cells were treated with 1 mM SCK6 for 24, 48 and 72 h. Cells were lysed in extraction buffer containing 50 mM Tris, pH 7.4, 0.3% 2-mercaptoethanol, 5 mM EDTA, 10 mM EGTA 5 μg/ml leupeptin, 5 μg/ml aprotinin, 10 μg/ml soybean trypsin inhibitor, 0.2 mM phenylmethyl-sulfonylfluoride. After 30 min of incubation on ice, cells were homogenized with a Dounce homogenizer, the homogenate was centrifuged at $100{,}000 \times g$ for 30 min at 4 °C, and supernatant (cytosolic fraction) was collected and analyzed by Western blotting for cytochrome *c* (Uehara et al., 1999).

2.9. Data analysis

All data are presented in this report as means ± S.D. of nine replicates from three independent experiments. Statistical differences were evaluated using the Student's *t*-test and considered significant at $P<0.05$, $P<0.01$ or $P<0.001$ level. Figures shown in this article were obtained from at least three independent experiments with similar results.

3. Results

3.1. Antipoliferative effect of SCK6

Phenylacetate had a strong antiproliferative effect and anti-tumor activity against several cancer cell lines at millimolar concentrations (Samid et al., 1992a,b; Ferrandina et al., 1997). In this study, six phenylacetate derivatives (SCK1–SCK6) with different alkyl chain lengths (the structures of these phenylacetate derivatives are illustrated in Fig. 1) were tested to examine their antiproliferative effects on human lung squamous carcinoma CH27 cells. As indicated in Fig. 2, treatment of CH27 cells with various concentrations (0.02, 0.2 and 2 mM) of phenylacetate or SCK1–SCK6 caused a dose-dependent decrease in cell number relative to control cultures. SCK6 was the most potent drugs, with an IC_{50} less than 0.4 mM (Fig. 3A,B).

3.2. Effect of SCK6 on cell cycle distribution

A previous report indicated that phenylacetate arrests human cancer cells in G_0/G_1 phase (Miller et al., 1997). To determine whether SCK6 also displays the same spectrum of cell cycle arrest activity, CH27 cells were treated with 1 mM SCK6 for 0, 8, 24 and 48 h. As show in Table 1, exposure of CH27 cells to SCK6 resulted in a significant

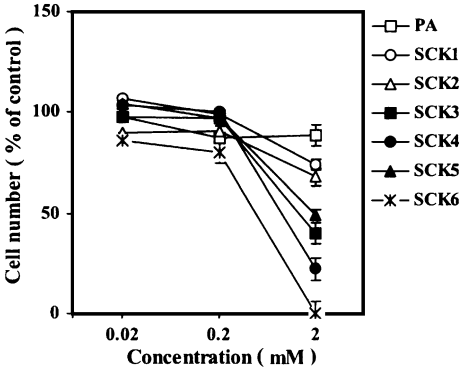

Fig. 2. Effects of phenylacetate and different phenylacetamides on cell growth. CH27 cells were treated with phenylacetate and *N*-alkyl-2-(2-fluorophenyl)acetamides for 4 days. Cell number was measured by Trypan blue dye exclusion method and the percentage of cell growth was calculated as a ratio of drug-treated cells and control cells (treated with 0.5% DMSO vehicle).

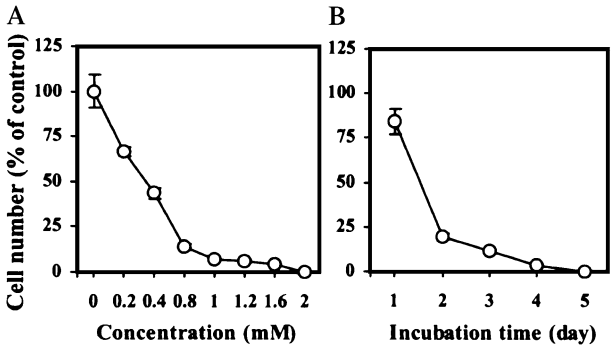

Fig. 3. Antiproliferative effect of SCK6 in CH27 cells. (A) Dose-dependent response. Cells were incubated with various concentrations of SCK6 for 3 days. (B) Time-course response. Cells were treated with 1 mM SCK6 for the indicated times. After incubation, cell number was determined by Trypan blue dye exclusion method.

increase in cells in G_1 phase, accompanied by a decrease in the percentage of cells in S phase. The SCK6-induced G_1 blockade peaked at 48 h, with approximately 85.9% of the cells in G_1 at that time compared with 64.5% in controls. However, 1 mM phenylacetate-treated or untreated control CH27 cells showed no significant change in cell cycle distribution.

3.3. Regulation of G_1 cell cycle regulatory proteins by SCK6

To determine the molecular mechanisms of SCK6-mediated G_1 arrest, we examined the expression of G_1-associated proteins in CH27 cells after SCK-6 treatment. As shown in Fig. 4, after 8 h of SCK6 treatment, CH27 cells showed a significant increase in p53 and $p21^{CIP1/WAF1}$ protein levels, which gradually increased up to 48 h. In contrast, levels of Cdk2, Cdk4, Cyclin A, Cyclin E and Cyclin D3 were markedly decreased in SCK6-treated CH27 cells in comparison with controls and phenylacetate-treated cells (Fig. 4).

Table 1
Cell cycle analysis of phenylacetate- and SCK6-treated CH27 cells

Time (h)	Cell cycle	Treatment (percentage of the cell number)		
		Control	Phenylacetate	SCK6
0	G_1	63.5 ± 3.4		
	S	28.1 ± 1.6		
	G_2/M	8.4 ± 2.1		
8	G_1	66.1 ± 2.4	59.7 ± 0.3	66.2 ± 1.0
	S	28.1 ± 3.5	32.3 ± 3.8	30.1 ± 2.0
	G_2/M	5.8 ± 2.3	10.3 ± 2.5	3.7 ± 2.2
24	G_1	67.3 ± 0.8	61.0 ± 0.5	71.0 ± 0.3
	S	26.4 ± 1.2	29.9 ± 0.9	24.3 ± 0.8
	G_2/M	6.3 ± 0.5	9.2 ± 0.5	4.6 ± 1.1
48	G_1	64.7 ± 2.5	63.3 ± 0.8	85.6 ± 1.3
	S	29.0 ± 2.7	31.1 ± 1.2	10.5 ± 1.3
	G_2/M	6.3 ± 0.8	5.6 ± 1.7	3.9 ± 0.2

The data are presented as means ± S.D. from one representative experiment ($n=3$). Similar results were obtained in three other independent experiments.

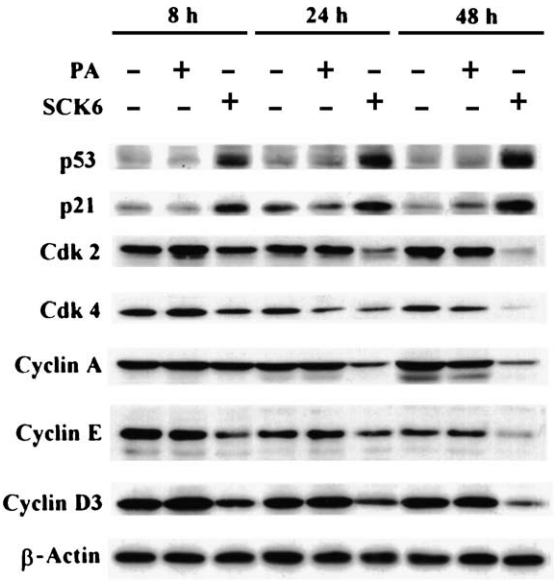

Fig. 4. Expression of cell cycle regulatory proteins. Cells were treated with vehicle or 1 mM SCK6 for the indicated times. After treatment, whole cell protein extracts were prepared as described in Materials and methods. Equal amounts of total proteins were resolved on SDS-polyacrylamide gels. Western blot analysis was performed using specific antibodies against proteins. Blots were re-probed for β-Actin to normalize each lane for protein content.

However, the pRb, Cdk6, Cyclin D1 and Cyclin D2 proteins are constitutively expressed, and no changes in their levels were observed during cell growth arrest caused by SCK6 treatment. These results indicate that the increase in p53 and $p21^{CIP1/WAF1}$ and decrease in Cdk2, Cdk4, Cyclin A, Cyclin E and Cyclin D3 might be involved in SCK6-mediated G_1 arrest.

3.4. Induction of apoptosis by SCK6

Phase-contrast microscopic examination of SCK6-treated CH27 cells showed that cells rounded up and detached from the culture plates after 48 to 72 h of incubation. This indicated that the antiproliferative effects of SCK6 might result in an earlier cell cycle G_1 arrest, followed by cell death. To characterize the cell death induced by SCK6, the nuclear morphology of dying cells was examined with a fluorescent DNA-binding agent, DAPI. CH27 cells treated with SCK6 displayed typical morphological features of apoptotic cells, with condensed and fragmented nuclei (Fig. 5A). Homogeneous nuclear chromatin was evident in control cells (treated with vehicle: 0.25% DMSO) and phenylacetate-treated cells. To confirm the morphological finding, in situ TUNEL assay and DNA fragmentation analysis were performed. As show in Fig. 5A, TUNEL-positive cells (apoptotic cells) and internucleosomal DNA fragments (Fig. 5B) were observed after SCK6 treatment. In control cultures, neither apoptotic cells nor DNA fragmentation was detected throughout the 72-h culture period.

3.5. Regulation of Bcl-2 family proteins by SCK6

Many lines of evidence demonstrated that Bcl-2-related proteins play an important role in either inhibition or promotion of apoptosis (Baliga and Kumar, 2002). To clarify whether the expression of these cell death-associated molecules is involved in SCK6-mediated apoptosis, CH27 cells were incubated with 1 mM phenylacetate or SCK6 for 24, 48 and 72 h. Results from Western blot analysis showed that exposure of CH27 cells to SCK6 caused a significant decrease in Bcl-2 protein level after 48 h of treatment (Fig. 6A), and a decrease in Bcl-X_L protein level was observed after 72 h of SCK6 treatment. However, there was no change in the level of Bax protein after SCK6 treatment. These results suggest that SCK6-induced apoptosis may be

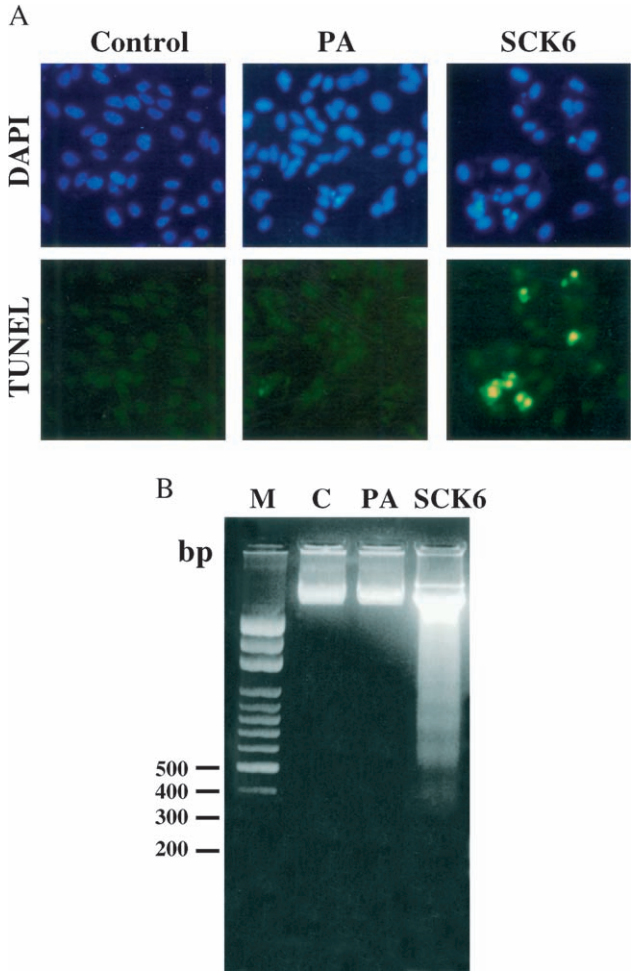

Fig. 5. Induction of apoptosis by SCK6. CH27 cells were treated with 0.25% DMSO as vehicle control or treated with 1 mM of SCK6 for 3 days. Cells were harvested and washed with ice-cold PBS, followed by fixation in 2% paraformaldehyde/PBS for 30 min. Cells were permeabilized in 0.1% Triton X-100/PBS for another 30 min, and then washed with distilled water. (A) Cells were treated with 1 μg/ml DAPI, or TUNEL reaction mixture and stained cells were examined using fluorescence microscopy. (B) DNA fragmentation. Cells were treated with phenylacetate and SCK6 for 3 days. Cellular DNA was extracted and analyzed by agarose gel electrophoresis.

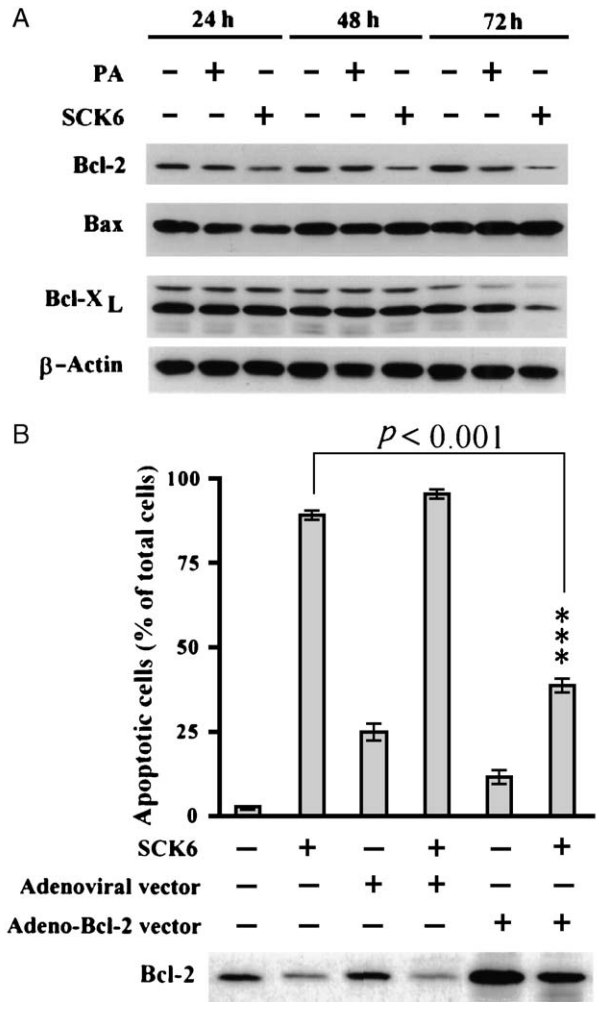

Fig. 6. Involvement of Bcl-2 in SCK6-induced apoptosis. (A) Western blot analysis of Bcl-2 family members. Cells were treated with vehicle or 1 mM SCK6 for the indicated times. After treatment, whole cell protein extracts were prepared as described in Materials and methods. Equal amounts of total proteins were resolved on SDS-polyacrylamide gels. Western blot analysis was performed using specific antibodies against Bcl-2, Bcl-X_L and Bax proteins. Blots were re-probed for β-Actin to normalize each lane for protein content. (B) Inhibition of SCK6-induced apoptosis by Bcl-2 overexpression. CH27 cells were infected with control adenoviral vector or adeno-Bcl-2 vector for 4 h, and then treated with vehicle or 1 mM SCK6 for another 72 h. After treatment, apoptotic cells were estimated using in situ TUNEL assay, and the cellular content was determined by Western blot assay.

mediated through the downregulation of Bcl-2 and Bcl-X_L anti-apoptotic proteins in CH27 cells. To elucidate whether the decrease in Bcl-2 protein was involved in SCK6-induced apoptosis, CH27 cells were infected with 50 multiplicity of infection (moi) adeno-Bcl-2 viral vector or control adenoviral vector. The expression of Bcl-2 protein was analyzed by Western blotting assay and the resulting cytotoxicity was estimated. As indicated in Fig. 6B, Bcl-2 protein level was increased by adeno-Bcl-2 infection but not by control adenoviral vector infection. In addition, overexpression of Bcl-2 protein by adeno-Bcl-2 infection significantly pro-

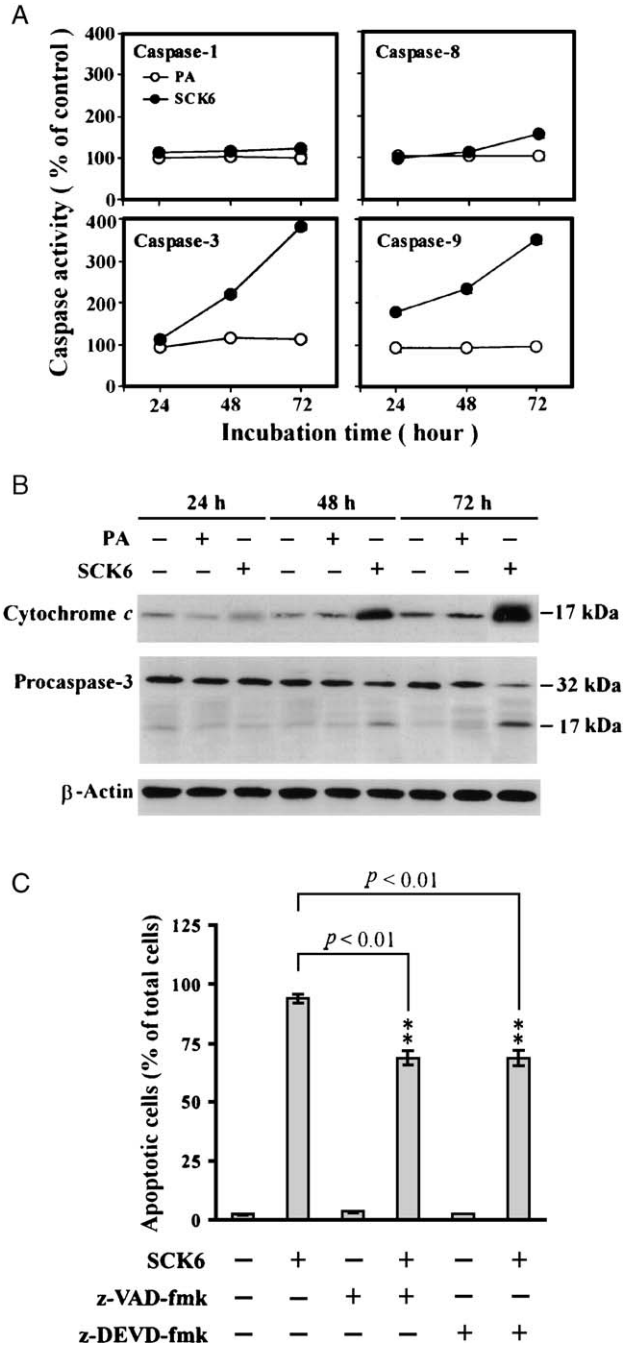

Fig. 7. Involvement of the caspase cascade in SCK6-induced apoptosis. (A) Activation of caspases by SCK6. Cells were treated with phenylacetate and SCK6 for different times or treated with 0.25% DMSO as vehicle control. Cell lysates were prepared and enzymatic activity of caspase-1, caspase-3-, caspase-8- and caspase-9-like proteases was determined by incubation of 200 μg of total protein with fluorogenic substrates, Ac-YVAD-AMC, Ac-DEVD-AMC, Ac-IETD-AMC and Ac-LEHD-AMC, respectively, for 2 h at 37 °C. The release of AMC was monitored spectrofluometrically (excitation = 360 nm; emission = 460 nm). (B) Determination of cytosolic cytochrome *c* and caspase-3. The cytosolic cell lysates were analyzed by Western blot using anti-cytochrome *c* and anti-caspase-3 specific antibodies. (C) Effects of caspase inhibitor on SCK6-induced apoptosis. Cells were pretreated with the broad-spectrum caspase inhibitor z-VAD-fmk for 1 h, and then stimulated with phenylacetate or SCK6. Apoptotic cells were determined by in situ TUNEL assay.

tected CH27 cells against SCK6-induced apoptotic death (Fig. 6B).

3.6. SCK6-induced apoptotic cell death via caspase activation

Caspases play a central role in the commitment to apoptosis after treatment with various drugs (Nieves-Neira and Pommier, 1999). To determine whether caspase activation is a downstream effector in SCK6-triggered apoptosis, fluorogenic substrates were used to detect specific caspase activity. As shown in Fig. 7A, caspase-9 specific activity drastically increased after 24 h of SCK6 treatment, and peaked at 72 h. In addition, SCK6 also caused a significant increase in caspase-3 activity (after 48-h treatment) and a slight increase in caspase-8 activity (after 72-h treatment), whereas the activity of caspase-1 was not affected by SCK6. Western blot analysis of the caspase-3 protein also showed that a 17-kDa active fragment of caspase-3 was detected after 48 and 72 h of SCK6 treatment (Fig. 7B). In addition, SCK6 caused a time-dependent accumulation of cytosolic cytochrome *c* protein. These results indicated that caspases were activated during SCK6-induced apoptosis. To clarify whether the activation of caspases was required for the induction of apoptotic death induced by SCK6, CH27 cells were co-treated with caspase inhibitor and SCK6. Result showed that incubation with a caspase-3 inhibitor (z-DEVD-fmk) or a broad-spectrum caspase inhibitor (z-VAD-fmk) markedly inhibited SCK6-mediated caspase-3 activation (data not shown) and apoptotic cell death (Fig. 7C). In contrast, caspase-1 inhibitor (z-YVAD-fmk) had no effect at a similar concentration (data not shown). These observations clearly indicated that the caspase cascade is crucially involved in SCK6-induced apoptosis.

4. Discussion

Phenylacetate was previously shown to reduce the malignant phenotype of promyelocytic leukemia, prostate cancer and glioblastoma cells (Samid et al., 1992b, 1994). The ability of phenylacetate to selectively arrest tumor growth and promote differentiation was confirmed using rats with a malignant brain tumor (Samid et al., 1994). In this article, we screened the activity of phenylacetate and its synthetic analogues, and found that SCK6 had a more potent antiproliferative activity in the human lung squamous carcinoma CH27 cell line than phenylacetate and other tested phenylacetate analogues. Our data show that SCK6 causes cell growth inhibition, cell cycle arrest and induction of apoptosis in a time- and dose-dependent manner in human lung squamous carcinoma CH27 cells.

Cell cycle analysis revealed G_1 arrest of CH27 cells after exposure to 1 mM of SCK6, and this G_1 arrest was accompanied by a dramatic decrease in the number of cells in S phase. A previous report has shown that phenylacetate-induced growth arrest is associated with p53-independent expression of $p21^{CIP1/WAF1}$ in human breast carcinoma MCF-7 cells (Gorospe et al., 1996). In this study, a marked increase in the cellular content of p53 and in the expression of $p21^{CIP1/WAF1}$ was observed in SCK6-treated CH27 cells. Cyclin-dependent kinases (Cdks), the heart of the eukaryotic cell cycle engine, are a family of serine/theronine protein kinases (Sherr and Roberts, 1995), and the activity of Cdks is regulated by $p21^{CIP1/WAF1}$. In SCK6-treated CH27 cells, accumulated $p21^{CIP1/WAF1}$ protein may bind to and inhibit the kinase activity of Cdk2, Cdk4 and Cdk6, therefore, preventing cells from entering the S phase and subsequently arresting the cell cycle in the G_1 phase. Moreover, the present study also showed that treatment with SCK6 markedly downregulated the expression of Cdk2, Cdk4 and Cyclin A, Cyclin D3 and Cyclin E proteins. It has been well documented that Cdk4 and Cdk6 are activated in association with D-type cyclin in the mid G_1 phase (Agami and Bernards, 2002), and Cdk2 is associated with cyclin E in the late G_1 phase and its activity is rate-limiting for progression from the G_1 to the S phase (Baldin et al., 1993; Tsai et al., 1993). Thus, reduced levels of these G_1-associated Cdks and cyclins may also facilitate blockade of the cell cycle in mid G_1 and G_1/S in SCK6-treated cells (Bartkova et al., 1997).

Accumulating evidence indicates that chemotherapeutic agents induce tumor regression through inhibition of proliferation and/or activation of apoptosis. Here, we demonstrated that SCK6 elicits apoptotic cell death as characterized by morphological changes, chromatin condensation and internucleosomal DNA fragmentation, accompanied by Bcl-2 downregulation, cytosolic cytochrome *c* accumulation and caspase activation. The family of Bcl-2-related proteins regulates susceptibility to apoptosis. Antiapoptotic members of the Bcl-2 family, including Bcl-2 and Bcl-X_L, act to prevent or delay cell death, while proapoptotic members, including Bax and Bcl-X_S, promote apoptosis (Reed, 1997). Our data showed that the expression of Bcl-2 proteins was decreased after 48 and 72 h of SCK6 treatment. In contrast, negligible change was noted in the expression of Bax protein. Overexpression of Bcl-2, induced by adeno-Bcl-2 vector infection, markedly inhibited SCK6-mediated apoptosis, suggesting that downregulation of Bcl-2 is involved in the apoptotic process. Previous studies have demonstrated that Bcl-2 expression can be altered in a variety of other cancers through various mechanisms, including loss of p53 tumor suppressor, which downregulates Bcl-2 expression in some tissues (Froesch et al., 1999; Reed et al., 1996). These results may indicate a possible role of p53 protein in downregulating Bcl-2 expression and may explain the induction of apoptosis by p53 protein in SCK6-treated cells. It has been reported that Bax is upregulated by p53 protein. Here, we could not detect any change in Bax protein after SCK6 treatment.

Previous reports (Earnshaw et al., 1999) have demonstrated that there are two pathways of caspase activation.

One involves the mitochondrial release of cytochrome *c* into the cytosol, where it binds the scaffolding protein apoptotic protease-activating factor-1 (Apaf-1), which in turn binds and activates the zymogen form of caspase-9. Once activated, caspase-9 can proteolytically activate caspases-3 and -7. The other caspase activation pathway involves ligation of death receptors followed by binding of the adaptor molecule Fas-activated death domain (FADD), which in turn binds and activates the zymogen form of caspase-8. Once activated, caspase-8 can cleave caspase-3, thereby leading to downstream events. In this study, the results presented in Figs. 6 and 7 showed that SCK6 reduced Bcl-2 and Bcl-X_L protein expression, increased cytosolic cytochrome *c* accumulation and subsequently induced activation of caspases-9 and -3. Overexpression of Bcl-2 and treatment with caspase inhibitor significantly prevented SCK6-induced apoptosis in CH27 cells. These observations clearly suggest that the mitochondrial-mediated caspase cascade is involved in SCK6-induced apoptosis.

In conclusion, the schematic representation of SCK6-triggered G_1 cell cycle arrest and the subsequent apoptotic cascade is described as following. Treatment of human lung cancer CH27 cells with SCK6 induced upregulation of p53 and $p21^{CIP1/WAF1}$ proteins and downregulation of G_1-related CDKs and cyclins, which blocked the cell cycle at the G_1 phase. This coincided with a decrease in Bcl-2 and Bcl-X_L protein levels and was followed by cytochrome *c*-triggered caspase-9 and caspase-3 activation and the onset of apoptosis. Taken together, our observations indicate that the antiproliferative effect of SCK6 in human lung CH27 cells is related to a multifaceted attack on multiple target proteins that are critically involved in cell cycle progression. Furthermore, SCK6-mediated Bcl-2 and Bcl-X_L downregulation, induced cytochrome *c* release from mitochondria to cytosol, and triggered activation of the caspase-9 cascade, suggesting that SCK6-induced apoptosis is via a mitochondrial pathway.

Acknowledgements

This work was supported by grants from China Medical College (CMC86-CM-21), Taichung Veterans General Hospital (TCVGH 897313D).

References

Agami, R., Bernards, R., 2002. Convergence of mitogenic and DNA damage signaling in the G1 phase of the cell cycle. Cancer Lett. 177, 111–118.

Baldin, V., Lukas, J., Marcote, M.J., Pagano, M., Draetta, G., 1993. Cyclin D1 is a nuclear protein required for cell cycle progression in G1. Genes Dev. 7, 812–821.

Baliga, B.C., Kumar, S., 2002. Role of Bcl-2 family of proteins in malignancy. Hematol. Oncol. 20, 63–74.

Bartkova, J., Lukas, J., Bartek, J., 1997. Aberrations of the G1- and G1/S-regulating genes in human cancer. Prog. Cell Cycle Res. 3, 211–220.

Brugarolas, J., Chandrasekaran, C., Gordon, J.I., Beach, D., Jacks, T., Hannon, G.J., 1995. Radiation-induced cell cycle arrest compromised by p21 deficiency. Nature 377, 552–557.

Brusilow, S.W., Danney, M., Waber, L.J., Batshaw, M., Burton, B., Levitsky, L., Roth, K., McKeethren, C., Ward, J., 1984. Treatment of episodic hyperammonemia in children with inborn errors of urea synthesis. N. Engl. J. Med. 310, 1630–1634.

Cinatl, J., Cinatl, J., Mainke, M., Weissflog, A., Rabenau, H., Kornhuber, B., Doerr, H.W., 1993. In vitro differentiation of human neuroblastoma cells induced by sodium phenylacetate. Cancer Lett. 70, 15–24.

Cinatl, J., Cinatl, J., Herneiz, P., Rabenau, H., Hovak, M., Benda, R., Gumbel, H.O., Kornhuber, B., Doerr, H.W., 1994. Induction of myogenic differentiation in a human rhabdomyosarcoma cell line by phenylacetate. Cancer Lett. 78, 41–48.

Cosentini, E., Haberl, I., Pertschy, P., Teleky, B., Mallinger, R., Baumgartner, G., Wenzl, E., Hamilton, G., 2001. The differentiation inducers phenylacetate and phenylbutyrate modulate camptothecin sensitivity in colon carcinoma cells in vitro by intracellular acidification. Int. J. Oncol. 19, 1069–1074.

Dubrez, L., Goldwasser, F., Genne, P., Pommier, Y., Solary, E., 1995. The role of cell cycle regulation and apoptosis triggering in determining the sensitivity of leukemic cells to topoisomerase I and II inhibitors. Leukemia 9, 1013–1024.

Earnshaw, W.C., Martins, L.M., Kaufmann, S.H., 1999. Mammalian caspases: structure, activation, substrates, and functions during apoptosis. Ann. Rev. Biochem. 68, 383–424.

Ferrandina, G., Melichar, B., Loercher, A., Verschraegen, C.F., Kudelka, A.P., Edwards, C.L., Scambia, G., Kavanagh, J.J., Abbruzzese, J.L., Freedman, R.S., 1997. Growth inhibitory effects of sodium phenylacetate (NSC 3039) on ovarian carcinoma cells in vitro. Cancer Res. 57, 4309–4315.

Froesch, B.A., Aime-Sempe, C., Leber, B., Andrews, D., Reed, J.C., 1999. Inhibition of p53 transcriptional activity by Bcl-2 requires its membrane-anchoring domain. J. Biol. Chem. 274, 6469–6475.

Gore, S.D., Samid, D., Weng, L.J., 1997. Impact of the putative differentiating agents sodium phenylbutyrate and sodium phenylacetate on proliferation, differentiation, and apoptosis of primary neoplastic myeloid cells. Clin. Cancer Res. 3, 1755–1762.

Gorospe, M., Shack, S., Guyton, K.Z., Samid, D., Holbrook, N.J., 1996. Up-regulation and functional role of p21Waf1/Cip1 during growth arrest of human breast carcinoma MCF-7 cells by phenylacetate. Cell Growth Differ. 7, 1609–1615.

Hudgins, W.R., Shack, S., Myers, C.E., Samid, D., 1995. Cytostatic activity of phenylacetate and derivatives against tumor cells. Correlation with lipophilicity and inhibition of protein prenylation. Biochem. Pharmacol. 50, 1273–1279.

Hunter, T., 1993. Braking the cycle. Cell 75, 839–841.

Kotas, M., Willner, J., Flentje, M., 2001. Sequential chemo-radiotherapy in non-small cell lung cancer. Lung Cancer 33 (Suppl. 1), S61–S64.

Miller, A.C., Whittaker, T., Thibault, A., Samid, D., 1997. Modulation of radiation response of human tumour cells by the differentiation inducers, phenylacetate and phenylbutyrate. Int. J. Radiat. Biol. 72, 211–218.

Nieves-Neira, W., Pommier, Y., 1999. Apoptotic response to camptothecin and 7-hydroxystaurosporine (UCN-01) in the 8 human breast cancer cell lines of the NCI Anticancer Drug Screen: multifactorial relationships with topoisomerase I, protein kinase C, Bcl-2, p53, MDM-2 and caspase pathways. Int. J. Cancer 82, 396–404.

Onishi, T., Yamakawa, K., Franco, O.E., Suzuki, R., Kawamura, J., 2000. p27Kip1 is the key mediator of phenylacetate induced cell cycle arrest in human prostate cancer cells. Anticancer Res. 20, 3075–3081.

Reed, J.C., 1997. Bcl-2 family proteins: regulators of apoptosis and chemoresistance in hematologic malignancies. Semin. Hematol. 34, 9–19.

Reed, J.C., Miyashita, T., Takayama, S., Wang, H.G., Sato, T., Krajewski, S., Aime-Sempe, C., Bodrug, S., Kitada, S., Hanada, M., 1996. BCL-2 family proteins: regulators of cell death involved in the pathogenesis of cancer and resistance to therapy. J. Cell. Biochem. 60, 23–32.

Samid, D., Shack, S., Sherman, L.T., 1992a. Phenylacetate: a novel nontoxic inducer of tumor cell differentiation. Cancer Res. 52, 1988–1992.

Samid, D., Yeh, A., Prasanna, P., 1992b. Induction of erythroid differentiation and fetal hemoglobin production in human leukemic cells treated with phenylacetate. Blood 80, 1576–1581.

Samid, D., Shack, S., Myers, C.E., 1993. Selective growth arrest and phenotypic reversion of prostate cancer cells in vitro by nontoxic pharmacological concentrations of phenylacetate. J. Clin. Invest. 91, 2288–2295.

Samid, D., Ram, Z., Hudgins, W.R., Shack, S., Liu, L., Walbridge, S., Oldfield, E.H., Myers, C.E., 1994. Selective activity of phenylacetate against malignant gliomas: resemblance to fetal brain damage in phenylketonuria. Cancer Res. 54, 891–895.

Sandler, M., Ruthven, C.R., Goodwin, B.L., Lees, A., Stern, G.M., 1982. Phenylacetic acid in human body fluids: high correlation between plasma and cerebrospinal fluid concentration values. J. Neurol. Neurosurg. Psychiatry 45, 366–368.

Semik, M., Schmid, C., Trosch, F., Broermann, P., Scheld, H.H., 2001. Lung cancer surgery-preoperative risk assessment and patient selection. Lung Cancer 33 (Suppl. 1), S9–S15.

Sherr, C.J., 1993. Mammalian G1 cyclins. Cell 73, 1059–1065.

Sherr, C.J., Roberts, J.M., 1995. Inhibitors of mammalian G1 cyclin-dependent kinases. Genes Dev. 9, 1149–1163.

Sidell, N., Wada, R., Han, G., Chang, B., Shack, S., Moore, T., Samid, D., 1995. Phenylacetate synergizes with retinoic acid in inducing the differentiation of human neuroblastoma cells. Int. J. Cancer 60, 507–514.

Simell, O., Sipila, I., Rajantie, J., Valle, D.L., Brusilow, S.W., 1986. Waste nitrogen excretion via amino acid acylation: benzoate and phenylacetate in lysinuric protein intolerance. Pediatr. Res. 20, 1117–1121.

Thibault, A., Cooper, M.R., Figg, W.D., Venzon, D.J., Sartor, A.O., Tompkins, A.C., Weinberger, M.S., Headlee, D.J., McCall, N.A., Samid, D., 1994. A phase I and pharmacokinetic study of intravenous phenylacetate in patients with cancer. Cancer Res. 54, 1690–1694.

Thibault, A., Samid, D., Cooper, M.R., Figg, W.D., Tompkins, A.C., Patronas, N., Headlee, D.J., Kohler, D.R., Venzon, D.J., Myers, C.E., 1995. Phase I study of phenylacetate administered twice daily to patients with cancer. Cancer 75, 2932–2938.

Tsai, L.H., Lees, E., Faha, B., Harlow, E., Riabowol, K., 1993. The cdk2 kinase is required for the G1-to-S transition in mammalian cells. Oncogene 8, 1593–1602.

Uehara, T., Kikuchi, Y., Nomura, Y., 1999. Caspase activation accompanying cytochrome *c* release from mitochondria is possibly involved in nitric oxide-induced neuronal apoptosis in SH-SY5Y cells. J. Neurochem. 72, 196–205.

Vaux, D.L., Korsmeyer, S.J., 1999. Cell death in development. Cell 96, 245–254.

Wang, J.L., Liu, D., Zhang, Z.J., Shan, S., Han, X., Srinivasula, S.M., Croce, C.M., Alnemri, E.S., Huang, Z., 2000. Structure-based discovery of an organic compound that binds Bcl-2 protein and induces apoptosis of tumor cells. Proc. Natl. Acad. Sci. U. S. A. 97, 7124–7129.

Wu, L.R., 1998. Application of 3-dimensional conformal therapy for non-small cell lung cancer. Clin. Med. (R.O.C.) 41, 194–196.